

Structural, microstructural, and transport properties of highly oriented LaNiO₃ thin films deposited on SrTiO₃ (100) single crystal

G. P. Mambrini and E. R. Leite

LIEC, Departamento de Química, Universidade Federal de São Carlos, Rod. Washington Luiz, km 235, CP 676, CEP 13565-905, São Carlos, SP, Brazil

M. T. Escote

Centro de Engenharia, Modelagem e Ciências Sociais Aplicadas, Universidade Federal do ABC, Rua Catequese 242, CEP 09090-900, Santo André, SP, Brazil

A. J. Chiquito

Departamento de Física, Universidade Federal de São Carlos, Rod. Washington Luiz, km 235, CP 676, CEP 13565-905, São Carlos, SP, Brazil

E. Longo and J. A. Varela

Instituto de Química, Universidade Estadual Paulista – Araraquara, R. Prof. Francisco Degni, s/n, CEP 14801-907, Araraquara, SP, Brazil

R. F. Jardim

Instituto de Física, Universidade de São Paulo, CP 66318, CEP 05315-970, São Paulo, SP, Brazil

(Received 3 April 2007; accepted 1 July 2007; published online 23 August 2007)

Electrical conductive textured LaNiO₃/SrTiO₃ (100) thin films were successfully produced by the polymeric precursor method. A comparison between features of these films of LaNiO₃ (LNO) when heat treated in a conventional furnace (CF) and in a domestic microwave (MW) oven is presented. The x-ray diffraction data indicated good crystallinity and a structural orientation along the (*h*00) direction for both films. The surface images obtained by atomic force microscopy revealed similar roughness values, whereas films LNO-MW present slightly smaller average grain size (~80 nm) than those observed for LNO-CF (60–150 nm). These grain size values were in good agreement with those evaluated from the x-ray data. The transport properties have been studied by temperature dependence of the electrical resistivity $\rho(T)$ which revealed for both films a metallic behavior in the entire temperature range studied. The behavior of $\rho(T)$ was investigated, allowing to a discussion of the transport mechanisms in these films. © 2007 American Institute of Physics.

[DOI: [10.1063/1.2769349](https://doi.org/10.1063/1.2769349)]

I. INTRODUCTION

Thin films of perovskite oxides with low electrical resistivity have been extensively studied due to the fact that such a physical property makes them suitable electrodes for perovskite ferroelectric layers in thin film capacitors.^{1–4} The use of oxide electrodes with low electrical resistivity results in a pronounced decrease of fatigue, a limitation commonly observed when metal bottom electrodes are used. In fact, for Pb(Zr_xTi_{1-x})O₃ (PZT) films deposited on oxide electrodes, the number of cycles without fatigue was found to increase from 10⁶ to 10¹⁰ cycles^{2,3} when metallic-like bottom electrodes based on perovskite oxides are used. Within this context, several oxides with low electrical resistivity and perovskite crystal structure have been investigated such as La_{0.5}Sr_{0.5}CoO₃, SrRuO₃, and LaNiO₃ (LNO). All of them display very low values of electrical resistivity at room temperature, typically of $\rho \sim 10^{-4}$ Ω cm, and have been used to fabricate fatigue-free ferroelectric thin films.^{2–4} The LNO oxides crystallize in a perovskite structure with rhombohedral or pseudocubic distortion and lattice parameters $c \approx 0.546$ nm and $a \approx 0.384$ nm, respectively.¹ Their transport properties are also of interest and they display a metallic-like behavior in a wide range of temperature,

roughly from 1 to 1000 K. In addition to this, the perovskite LNO exhibits Pauli paramagnetism and does not undergo any phase transformation within this temperature interval.^{5,6}

Many efforts have been used for preparing LNO thin films by different deposition techniques such as sputtering,⁷ pulsed laser deposition,^{8,9} molecular beam epitaxy,¹⁰ metal-organic decomposition,¹¹ and sol-gel methods.¹² More recently, an alternative route, based on a method of chemical solution deposition, called complex polymerization route, has been successfully used for growing thin films of several oxides as, e.g., PZT,^{13,14} BaTiO₃,¹⁵ SrTiO₃,¹⁶ LiNbO₃,¹⁷ and LNO films.¹ In all cases, the complex polymerization route allowed the production of stoichiometric films with excellent structural and electrical properties.

As far as these previous studies are concerned, polycrystalline thin films were formed but without any appreciable preferred orientation. Then, one of the aims of this work is to study the experimental conditions to produce LNO thin films with a high degree of orientation. In fact, some changes in the experimental procedure can be made in order to obtain an oriented system. First of all, the LNO films can be deposited onto a preferred oriented single crystal, as LaAlO₃ or even SrTiO₃. This has been made, for example, by Bouquet *et al.*¹⁷ that obtained epitaxially growth of LiNbO₃ films on

sapphire substrate by the complex polymerization route. Another route to obtain highly oriented thin films is by using a domestic microwave oven during the crystallization process. Such a procedure has been successfully applied for depositing thin films of LiNbO_3 and $\text{SrBi}_2\text{Nb}_2\text{O}_9$ (Refs. 18 and 19). Also, LNO electrodes grown on LaAlO_3 (100) substrates, with (100) crystallographic orientation, were also obtained by performing the heat treatment of the thin films in a microwave oven.²⁰ By using a similar procedure, the same authors described the deposition of highly oriented $\text{Pb}_{1-x}\text{Ba}_x\text{TiO}_3$ films with excellent electrical properties.²⁰

We discuss here the general physical properties of highly oriented LaNiO_3 thin films grown by the complex polymerization method on SrTiO_3 (100) substrates. These films were characterized by structural, morphological, and electrical transport measurements. The thin films were heat treated in a conventional furnace and in a domestic microwave oven and their general physical properties were compared. We have also investigated the transport properties of these films, which allowed us a discussion concerning the transport mechanisms of these perovskite LaNiO_3 thin films.

II. EXPERIMENTAL PROCEDURE

LaNiO_3 thin films were deposited on SrTiO_3 (100) single crystal substrates by spin coating solution deposition of a polymeric precursor. Details of the method employed are described elsewhere.^{1,20,21} After the deposition, the films are preliminary heat treated at 300 °C in a conventional electric furnace in order to eliminate organic compounds and to obtain an amorphous and continuous inorganic film. The crystallization of these thin films was carried out in two different furnaces: (a) in a conventional electric furnace operating at 700 °C for 2 h and using a heating rate of 5 °C/min; and (b) in a domestic microwave oven at 700 °C for 10 min with a heating rate of 230 °C/min. The microwave furnace used in these experiments is similar to the one described in Ref. 18. The steps described previously were repeated until the films reached the desired thickness of ~200 nm. The samples heat treated in the conventional furnace and in the microwave oven are thereafter referred to as LNO-CF and LNO-MW, respectively.

The structural features of the LaNiO_3 thin films were analyzed by x-ray diffraction (XRD). These measurements were carried out in a Rigaku DMax 2500PC diffractometer by using $\text{Cu } K\alpha$ radiation and 2θ varying from 20° to 60°. The film thickness was inferred by direct observation of scanning electron microscopy (SEM) images of the cross section of the films in a Zeiss DSM940A microscope. Atomic force microscopy (AFM) was used to analyze the surface morphology of these films. The images were taken in a Digital Instruments Multi-Mode Nanoscope IIIA microscope. These images allowed an accurate analysis of important parameters as surface roughness and average grain size.

The temperature dependence of the electrical resistivity $\rho(T)$ of these films was measured by using the standard direct current four-probe method. Four copper electrical leads were attached with Ag epoxy onto the films surface. The measurements were performed in a homemade system with a

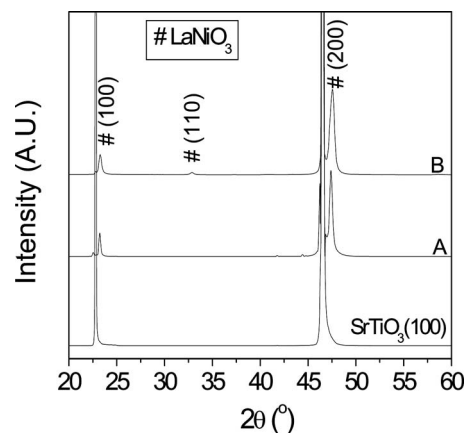


FIG. 1. X-ray diffraction patterns of the SrTiO_3 substrate: (a) LNO films crystallized in a conventional furnace and (b) LNO films crystallized on a microwave oven.

cold finger coupled to two multimeters and two current sources and in a temperature window from 20 to 300 K. The electrical resistivity was evaluated by considering the thickness values previously obtained by the SEM analysis.

III. RESULTS AND DISCUSSION

Figure 1 displays the x-ray patterns of oriented LaNiO_3 thin films deposited on SrTiO_3 (100) substrates and heat treated in: (a) a conventional furnace at 700 °C for 2 h and at a heat rate of 5 °C/min; and (b) a microwave oven at 700 °C for 10 min and at a heat rate of 230 °C/min. From the x-ray diagrams exhibited in Fig. 1, we have identified the Bragg reflections belonging to the perovskite LaNiO_3 phase in both samples, indicating that the thin films are single phase materials. The x-ray patterns also revealed a much higher intensity for the (100) and (200) reflections in both films, suggesting that they are aligned along the $(h00)$ orientation. A careful inspection of the x-ray data also indicates that both samples exhibit a reflection occurring at $2\theta \sim 33^\circ$. Such a peak, with rather low intensity, has been identified as belonging to the most intense reflection of the pattern taken in a polycrystalline LaNiO_3 specimen.¹ This peak, corresponding to the (110) Bragg plane, was found to be much more intense in the LNO-MW thin film, further indicating that a rather low heating rate combined with a prolonged heat treatment provide a better orientation of the crystallites within the material. In order to give support to this statement, the degree of preferred orientation F has been estimated by using the relationship first proposed by Lotgering:²²

$$F = \frac{P - P_0}{1 - P_0}, \quad (1)$$

where

$$P = \frac{\sum I(h00)}{\sum I(hkl)}, \quad (2)$$

I is the peak intensity, and P_0 is the P value for a polycrystalline sample (based on the JCPDS catalog). The F values were found to be 0.998(23) and 0.94(1) for samples LNO-CF

and LNO-MW, respectively, further indicating that prolonged heat treatments result in a higher degree of orientation of the LNO thin films. Such a result is in agreement with those reported elsewhere where a higher degree of orientation in LaNiO_3 films was observed when the film is subjected to prolonged heat treatments.¹² In fact, the results of x-ray indicated that LNO films prepared by a chemical solution method and heat treated at 700 °C for 5 and 10 h have $F = 0.91$ and 0.95, respectively.¹² The authors argued that a high degree of orientation would be a natural consequence of prolonged heat treatments which are responsible for a release of the internal stress, for a better alignment of nonoriented crystallites, and for the coalescence of grains within the film.²³

The x-ray data are also valuable for calculating the lattice parameter a , which was found to be $a \sim 0.383$ and 0.382 nm for LNO-CF and LNO-MW thin films, respectively. These values of a are in excellent agreement with that of $a = 0.383$ nm found in LNO films grown by pulsed laser ablation.²⁴ We have also estimated the average crystallite size of these films by using the Scherrer relation and the full width at half maximum of the diffraction peaks. The average crystallite sizes were ~ 100 and 30 nm for LNO-CF and LNO-MW thin films, respectively. For the LNO-CF film, such result is in good agreement with that of ~ 95 nm described in literature for LNO films deposited on Si (111) substrate.¹ The LNO-MW film was found to have a rather smaller crystallite size ~ 30 nm, a feature certainly related to the shorter period of time used for the heat-treatment, or more appropriated to the crystallization process by using the microwave furnace. Such a heat treatment seems to be insufficient to promote a complete crystallite growth.²⁵

The surface morphology of the films has been investigated by AFM and the results for both films are displayed in Fig. 2. Figures 2(a) and 2(b) are related to LNO-CF, whereas Figs. 2(c) and 2(d) correspond to the surface reconstruction of LNO-MW. These images indicate that both films display a smooth, homogeneous, and crack-free surface. Average roughness (RMS) values of ~ 4.3 and 12.4 nm have been obtained from the images of LNO-CF and LNO-MW, respectively. The result obtained for LNO-CF is comparable with RMS values of 3.7 nm and 5.5 nm reported in the literature for similar thin films.^{1,26}

The morphology of the grains can be observed in the images with higher magnification, as displayed in Figs. 2(b) and 2(d). A comparison between these figures discloses the influence of the heat treatment on the size and shape of the grains of the LaNiO_3 films. In fact, elongated grains, with typical length and width values of 150 and 60 nm, respectively, are observed in images belonging to the LNO-CF thin films, whereas those of LNO-MW films exhibit bigger grains with irregular shape and average radius close to 80 nm. Such average values of radius are in line with those of ~ 120 nm seen in LaNiO_3 thin films deposited on LaAlO_3 substrates.²⁰ We argue that such a difference in the morphologies may be related to the two different process of crystallization employed here. In any event, both methods provided textured films and prolonged times of heat treatment were found to promote grain growth by coalescence and, consequently, re-

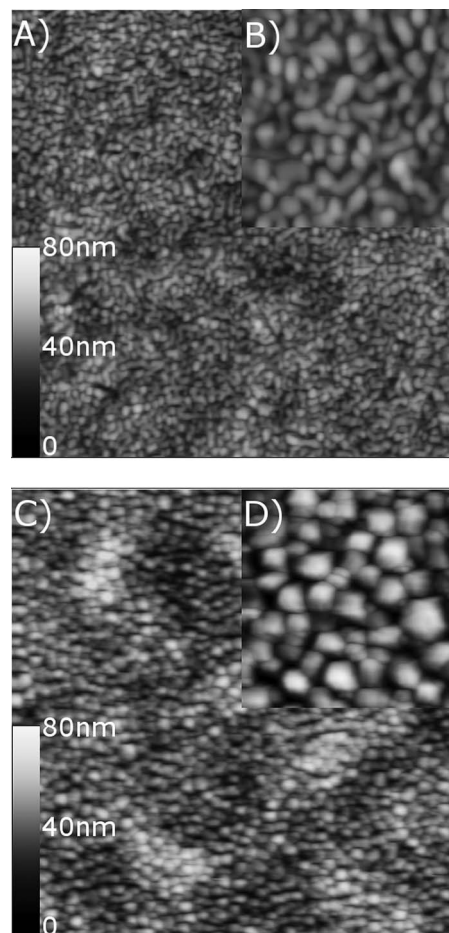


FIG. 2. AFM images of the LNO thin films. (a) and (b) Related to the surface reconstruction of the LNO-CF sample and (c) and (d) correspond to the LNO-MW thin film. (a) and (c) Low magnification ($5 \times 5 \mu\text{m}$) and (b) and (d) high magnification ($1 \times 1 \mu\text{m}$).

sulting in elongated grains and a smoother surface. Similar features have been observed in oriented $\text{YBa}_2\text{Cu}_3\text{O}_7$ thin films when subjected to different time intervals during the heat treatment.²⁵

Cross section analyses of these films were performed by SEM and revealed (not shown) that both samples display similar thickness of ~ 200 nm. However, we also mention that a critical thickness ~ 50 nm, for depositing LaNiO_3 thin films by pulsed laser ablation, has been proposed elsewhere.⁹ It was argued that films with thickness above this critical value would have cracked surfaces, a feature hardly seen in our thin films.

In order to study the transport properties of these thin films, measurements of electrical resistivity $\rho(T)$ versus temperature have been conducted and the relevant results are displayed in Fig. 3. The $\rho(T)$ curves reveal a monotonic decrease of $\rho(T)$ with decreasing temperature, a behavior typically found in metals.¹ However, a careful inspection of the data indicates that there are at least two different behaviors of $\rho(T)$ in the temperature range investigated: (a) at temperatures above ~ 100 K, where $\rho(T)$ is linear; and (b) at temperatures below 100 K, where $\rho(T)$ is larger than expected for a linear behavior. Similar $\rho(T)$ behaviors have been frequently observed in LNO thin films and polycrystalline samples, as discussed elsewhere.^{1,27,28}

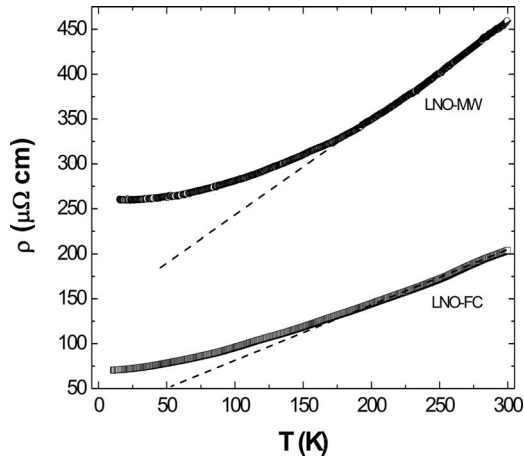


FIG. 3. Temperature dependence of the electrical resistivity of both samples: LNO-CF and LNO-MW. The dotted lines are guides to the eye.

A comparison between LNO-CF and LNO-MW $\rho(T)$ curves revealed a clear difference in the $\rho(T)$ values and, at $T < 200$ K, in the temperature-dependent resistivity data (see Fig. 3). In fact, values of ρ at 300 K were found to be $200 \mu\Omega \text{ cm}$ and $460 \mu\Omega \text{ cm}$ for the films LNO-CF and LNO-MW, respectively. These values of $\rho(T)$ are very low and further indicate that LNO thin films are excellent candidates for practical applications. In addition to this, they are in good agreement with $\rho(T=300 \text{ K}) \sim 300 \mu\Omega \text{ cm}$ reported in films of LNO produced by pulsed laser ablation⁸ and $\rho(T=300 \text{ K}) \sim 340 \mu\Omega \text{ cm}$ in thin films prepared by a sol-gel technique.¹² However, these values of $\rho(T=300 \text{ K})$ are much lower than that of $\sim 750 \mu\Omega \text{ cm}$ obtained for polycrystalline LNO films grown on Si (111) substrates by the complex polymerization method.¹

At low temperatures, or more appropriately at ~ 20 K, the ρ values were $72 \mu\Omega \text{ cm}$ (LNO-CF) and $259 \mu\Omega \text{ cm}$ (LNO-MW). This implies in residual resistivity ratios ($\rho_{300 \text{ K}}/\rho_{20 \text{ K}}$) of ~ 2.78 and ~ 1.77 for the film crystallized in the conventional furnace and for the film annealed in the microwave oven, respectively. The latter value of $\rho_{300 \text{ K}}/\rho_{20 \text{ K}}$ is essentially the same ($\rho_{300 \text{ K}}/\rho_{20 \text{ K}}=1.75$) found in LaNiO_3 films deposited on SrTiO_3 (100).²⁷

At temperatures above 200 K, the positive temperature-coefficient of the electrical resistivity, $[(1/\rho)d\rho/dT]$, was found to be 3.8×10^{-3} and $3.0 \times 10^{-3} \text{ K}^{-1}$ for LNO-CF and LNO-MW, respectively. These values of $(1/\rho)d\rho/dT$ are comparable to the ones found in ordinary metals like Cu, $(1/r)dr/dT \sim 4.4 \times 10^{-3} \text{ K}^{-1}$, and other values listed in literature of $2.4 \times 10^{-3} \text{ K}^{-1}$ for LaNiO_3 .^{27,28}

In order to further discuss the temperature dependence of the $\rho(T)$, the temperature ranges where $\rho(T)$ displays different behaviors were fitted assuming a power law:

$$\rho(T) = A + BT^n, \quad (3)$$

where A is the residual electrical resistivity, B is the temperature-dependent coefficient, and n ranges from 1 to 2. At this point, it is important to notice that the mechanism limiting the mean free path of the carriers in LNO compounds is certainly related to the bulk properties and not, e.g., to the grain boundary scattering.²⁹

At higher temperatures, or more appropriately from 200 to 300 K, the $\rho(T)$ curves for both samples were fitted to a linear expression: $\rho(T) = \rho_0 + AT$. Such a behavior of the $\rho(T)$ curves is typical of electron-phonon scattering, where ρ_0 is the residual electrical resistivity of the material and A is the temperature-dependent coefficient. The values of ρ_0 were ~ 35 and $\sim 145 \mu\Omega \text{ cm}$ for samples LNO-CF and LNO-MW, respectively. For the sample heat treated in the conventional furnace, the temperature dependence coefficient was $0.55 \mu\Omega \text{ cm/K}$, whereas $A \sim 1 \mu\Omega \text{ cm/K}$ was obtained for the sample crystallized in the microwave oven.

By assuming that the linear behavior of $\rho(T)$ data is related to the electron-phonon scattering, the electron-phonon coupling constant λ can be estimated by using the appropriate expression:^{30,31}

$$\lambda = \frac{\hbar \omega_p^2}{8\pi^2 k_B} A = 0.246(\hbar \omega_p)^2 A, \quad (4)$$

where \hbar is the Planck constant divided by 2π , ω_p is the plasma frequency, k_B is the Boltzmann constant, and A is the slope of the $\rho(T)$ curve ($\mu\Omega \text{ cm/K}$). Assuming that the plasmon energy $\hbar \omega_p \approx 1 \text{ eV}$, obtained for the LNO bulk when electron energy-loss experiments are considered,³² the electron-phonon coupling constant λ can be estimated for both films. The estimated values of λ are ~ 0.14 for LNO-CF and ~ 0.26 for LNO-MW. These values of λ are in good agreement with the one of $\lambda \approx 0.3$ found in polycrystalline samples of LaNiO_3 (Ref. 28) and further suggest a weak coupling between electrons and phonons in this compound.

The lack of saturation of $\rho(T)$ at 300 K for both films indicates that the mean free path l of the carriers is actually longer than the dimensions of the unit cell. An estimate of l , at temperatures in which the $\rho(T)$ data displays a linear behavior, can be obtained by using the relationship:^{30,31}

$$l = \frac{4.95 \times 10^{-4} v_F}{\rho(\hbar \omega_p)^2}, \quad (5)$$

where v_F is the Fermi velocity, which has been estimated to be $v_F \sim 1.05 \times 10^7 \text{ cm s}^{-1}$ for LaNiO_3 ,³³ and ω_p the plasma frequency $\hbar \omega_p \sim 1 \text{ eV}$. The values of l , at 300 K, were found to be ~ 31 and $\sim 15 \text{ \AA}$ for the LNO-CF and LNO-MW films, respectively. These values of l are much longer than the unit cell parameters obtained through the x-ray data of $\sim 3.8 \text{ \AA}$. In addition to this, the l values are comparable to $l \sim 15 \text{ \AA}$ obtained for polycrystalline samples of LaNiO_3 .²⁹ In the case of the LNO-CF film, the estimated l is almost twice longer than that reported for the bulk LNO. We argue that such difference in l can be related to the highly oriented nature of the LNO-CF thin film which results in lower scattering of the charge carriers. It is important to notice that some authors have observed isotropic transport properties of LaNiO_3 bulk samples.²⁹

For the LNO-CF thin film, the low temperature $\rho(T)$ data ($20 < T < 140 \text{ K}$) was found to be well described by Eq. (3) with $n=3/2$, where $A_{\text{CF}}=68.7 \mu\Omega \text{ cm}$ and $B_{\text{CF}}=0.0271 \mu\Omega \text{ cm/K}^{3/2}$. The best fit found for the $\rho(T)$ data is shown in Fig. 4. In Fig. 4, it is also shown that the $\rho(T)$ data of LNO-MW thin film, in the same temperature range, devi-

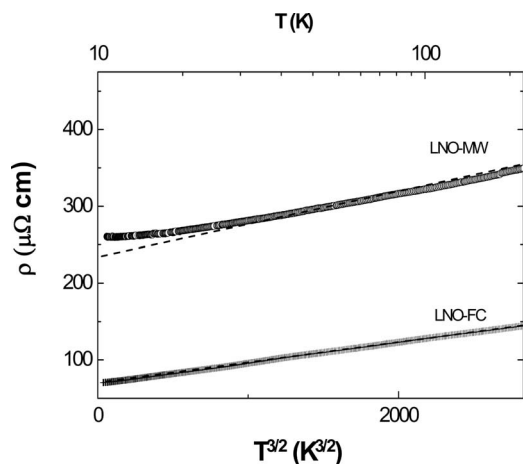


FIG. 4. $T^{3/2}$ dependence of the electrical resistivity of the sample LNO-FC and LNO-MW measured in the temperature range $10 < T < 200$ K.

ates from the $T^{3/2}$ behavior and seems to obey the expression $\rho(T) = A_{MW} + B_{MW}T^2$, as displayed in Fig. 5. We were able to fit the $\rho(T)$ data by using this equation with $A_{MW} = 258.2 \mu\Omega \text{ cm}$ and $B_{MW} = 0.0023 \Omega \text{ cm/K}^2$. In general, such a T^2 contribution term to $\rho(T)$ is ascribed to the electron–electron scattering, whereas a $T^{3/2}$ term is related to a combination of a T^2 contribution and an electron-phonon scattering resistivity T term.^{1,28} Also, the linear coefficient B_{MW} is useful to estimate the Kawakami–Woods ratio (r_{KW}) by using $r_{KW} \equiv B_{MW}/\gamma^2$, where γ is the electronic specific heat coefficient. When one assumes $\gamma \sim 13.8 \text{ mJ mol}^{-1} \text{ K}^{-2}$ for LNO, as reported elsewhere,³⁴ a value of $r_{KW} \sim 1.2 a_0$, with $a_0 \equiv 10 \mu\Omega \text{ cm mol}^2 \text{ K}^2 \text{ J}^{-2}$, is obtained. As discussed in Ref. 35, the ratio r_{KW} close to a_0 indicates strong electron correlations, further suggesting that such electron-electron scattering can be related to the proximity of a nearby Mott transition.

As far as the n - T -exponent is concerned, we first mention that some authors usually associate the magnitude of this exponent to the presence of defects within grains like oxygen vacancies or even extrinsic grain-boundaries contributions and porosity. However, our samples, based on the discussion made earlier, have similar microstructural features, oxygen stoichiometry, and porosity, and the origin of different values

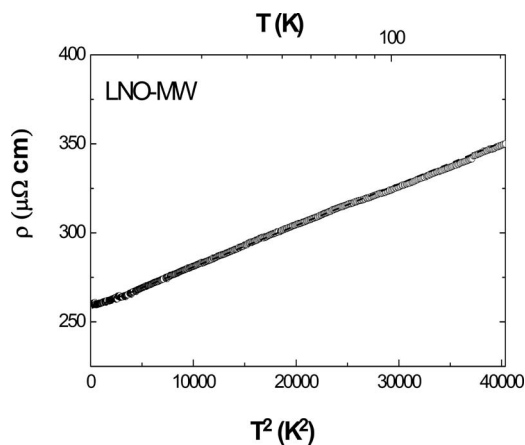


FIG. 5. T^2 dependence of the electrical resistivity of the sample LNO-MW measured in the temperature range $10 < T < 200$ K.

of n would be mainly related to the slight different preferred orientation degree or to the structural strains due to the rapid heat treatment made in the microwave oven. Despite the small differences observed on microstructural and transport properties of these films, the combination of structural, morphological, and transport characterizations revealed that the polymeric precursor method allowed to the production of textured single-phase LaNiO_3 thin films with uniform microstructure and excellent electrical properties.

IV. CONCLUSIONS

In summary, textured and single-phase $\text{LaNiO}_3/\text{SrTiO}_3$ (100) thin films were successfully produced by the polymeric precursor method. A comparison between the features of these films heat treated in a conventional furnace and in a domestic microwave oven has been made. The XRD analysis indicated a high degree of crystallinity and the structural orientation along the ($h00$) direction for both films. The surface images obtained by AFM revealed similar roughness values, whereas films LNO-MW have slight smaller average grain size (~ 80 nm) than those observed for LNO-FC (60–150 nm). Electrical resistivity measurements for both films displayed metallic behavior over the entire temperature range investigated (20–300 K). These measurements also revealed larger electrical resistivity values for LNO-MW films, although these differences may be related with both the high heating rate and the low crystallization time used during the heat treatment performed on the microwave oven. Below 150 K, the $\rho(T)$ curves were fitted by considering different temperature dependencies. For the LNO-MW films, the $\rho(T)$ data were fitted with a T^2 term; and for the LNO-FC films, $\rho(T)$ was adjusted to a $T^{3/2}$ term. The combined results suggested that the crystallization processes of LaNiO_3 thin films in microwave oven, as well as the crystallization in conventional furnace are promising routes for producing LNO thin films. In addition to this, the results discussed here make these films promising candidates for application as bottom electrodes in ferroelectric-based memory devices.

ACKNOWLEDGMENTS

The authors acknowledge the financial support from the Brazilian agencies FAPESP, CNPq, and CAPES. One of the authors (R.F.J.) acknowledges FAPESP under Grant No. 05/53241-9 and CNPq under Grant No. 303272/2004-0.

¹M. T. Escote, F. M. Pontes, E. R. Leite, J. A. Varela, R. F. Jardim, and E. Longo, *Thin Solid Films* **445**, 54 (2003).

²M. S. Chen, T. B. Wu, and J. M. Wu, *Appl. Phys. Lett.* **68**, 1430 (1996).

³B. G. Chae, Y. S. Yang, S. H. Lee, M. S. Jang, S. J. Lee, S. H. Kim, W. S. Baek, and S. C. Kwon, *Thin Solid Films* **410**, 107 (2002).

⁴C. Guerrero, F. Sánchez, C. Ferrater, J. Roldán, M. V. García-Cuenca, and M. Varela, *Appl. Surf. Sci.* **168**, 219 (2000).

⁵A. K. Raychaudhuri, *Adv. Phys.* **44**, 21 (1995).

⁶P. Lacorre, J. B. Torrance, J. Pannetier, A. I. Nazzari, P. W. Wang, and T. C. Huang, *J. Solid State Chem.* **91**, 225 (1991).

⁷N. Wakiya, T. Azuma, K. Shinozaki, and N. Mizutani, *Thin Solid Films* **410**, 114 (2002).

⁸F. Sánchez, C. Ferrater, C. Guerrero, M. V. García-Cuenca, and M. Varela, *Appl. Phys. A: Mater. Sci. Process.* **71**, 59 (2000).

⁹F. Sánchez, C. Ferrater, X. Alcóbé, J. Bassas, M. V. García-Cuenca, and M. Varela, *Thin Solid Films* **384**, 200 (2001).

- ¹⁰A. Y. Dobin, K. R. Nikolaev, I. N. Krivorotov, R. M. Wentzcovitch, E. D. Dahlberg, and A. M. Goldman, *Phys. Rev. B* **68**, 113408 (2003).
- ¹¹A. Li, C. Ge, P. Lu, and N. Ming, *Appl. Phys. Lett.* **68**, 1347 (1996).
- ¹²S. Miyake, S. Fujihara, and T. Kimura, *J. Eur. Ceram. Soc.* **21**, 1525 (2001).
- ¹³M. T. Escote, F. M. Pontes, E. R. Leite, E. Longo, R. F. Jardim, and P. S. Pizani, *J. Appl. Phys.* **96**, 2186 (2004).
- ¹⁴F. M. Pontes, E. R. Leite, M. S. J. Nunes, D. S. L. Pontes, E. Longo, R. Magnani, P. S. Pizani, and J. A. Varela, *J. Eur. Ceram. Soc.* **24**, 2969 (2004).
- ¹⁵E. J. H. Lee, F. M. Pontes, E. R. Leite, E. Longo, J. A. Varela, E. B. Araujo, and J. A. Eiras, *J. Mater. Sci. Lett.* **19**, 1457 (2000).
- ¹⁶F. M. Pontes, E. R. Leite, E. J. H. Lee, E. Longo, and J. A. Varela, *J. Eur. Ceram. Soc.* **21**, 419 (2001).
- ¹⁷V. Bouquet, M. I. B. Bernardi, S. M. Zanetti, E. R. Leite, E. Longo, J. A. Varela, M. G. Viry, and A. Perrin, *J. Mater. Res.* **15**, 2446 (2000).
- ¹⁸N. S. L. S. Vasconcelos, J. S. Vasconcelos, V. Bouquet, S. M. Zanetti, E. R. Leite, E. Longo, L. E. B. Soledade, F. M. Pontes, M. Guilloux-Viry, A. Perrin, M. I. Bernardi, and J. A. Varela, *Thin Solid Films* **436**, 213 (2003).
- ¹⁹J. S. Vasconcelos, N. S. L. S. Vasconcelos, S. M. Zanetti, E. R. Leite, J. A. Varela, and E. Longo, *Appl. Surf. Sci.* **225**, 156 (2004).
- ²⁰F. M. Pontes, E. R. Leite, G. P. Mambrini, M. T. Escote, E. Longo, and J. A. Varela, *Appl. Phys. Lett.* **84**, 248 (2004).
- ²¹M. T. Escote, F. M. Pontes, G. P. Mambrini, E. R. Leite, J. A. Varela, and E. Longo, *J. Eur. Ceram. Soc.* **25**, 2341 (2005).
- ²²T. Ami and M. Suzuki, *Mater. Sci. Eng., B* **54**, 84 (1998).
- ²³W. Lu, P. Zheng, W. Du, and Z. Meng, *J. Mater. Sci.: Mater. Electron.* **15**, 739 (2004).
- ²⁴K. M. Satyalakshmi, M. Mallya, K. V. Ramanathan, X. D. Wu, B. Brainard, D. C. Gautier, N. Y. Vasanthacharya, and M. S. Hedge, *Appl. Phys. Lett.* **62**, 1233 (1993).
- ²⁵X. M. Cui, B. W. Tao, J. Xiong, X. Z. Liu, J. Zhu, and Y. R. Li, *Physica C* **432**, 147 (2005).
- ²⁶A. Li, D. Wu, Z. Liu, C. Ge, X. Liu, G. Chen, and N. Ming, *Thin Solid Films* **336**, 386 (1998).
- ²⁷C. R. Cho, D. A. Payne, and S. L. Cho, *Appl. Phys. Lett.* **71**, 3013 (1997).
- ²⁸X. Q. Xu, J. L. Peng, Z. Y. Li, H. L. Ju, and R. L. Greene, *Phys. Rev. B* **48**, 1112 (1993).
- ²⁹N. Gayathri, A. K. Raychaudhuri, X. Q. Xu, J. L. Peng, and R. L. Greene, *J. Phys. Condens. Matter* **10**, 1323 (1998).
- ³⁰See, for example, M. T. Escote, V. B. Barbeta, R. F. Jardim, and J. Campo, *J. Phys.: Condens. Matter* **18**, 6117 (2006); M. T. Escote, V. A. Mesa, R. F. Jardim, L. Ben-Dor, M. S. Torikachvili, and A. H. Lacerda, *Phys. Rev. B* **66**, 144503 (2002).
- ³¹M. Gurvitch and A. T. Fiory, *Phys. Rev. Lett.* **59**, 1337 (1987).
- ³²J. P. Kemp and P. A. Cox, *Solid State Commun.* **75**, 731 (1990).
- ³³The v_F value can be estimated as follows: $v_F = \hbar(3\pi n)^{1/3}/m^*$, where $n = 1.7 \times 10^{22} \text{ cm}^{-3}$, by assuming one electron per Ni atom ($\text{Ni}^{3+}, t_{2g}^6 e_g^1$) (see Ref. 28).
- ³⁴K. Sreedhar, J. M. Honig, M. Darwin, M. McElfresh, P. M. Shand, J. Xu, B. C. Crooker, and J. Spalek, *Phys. Rev. B* **46**, 6382 (1992).
- ³⁵S. Y. Li, L. Taillefer, D. G. Hawthorn, M. A. Tanatar, J. Paglione, M. Sutherland, R. W. Hill, C. H. Wang, and X. H. Chen, *Phys. Rev. Lett.* **93**, 056401 (2004).